International Journal of Navigation and Port Research
Vol.27, No.6 pp. 625~630, 2003 (ISSN 1598 5725)

The Safety of Maneuverability Based on the Hydrodynamic Forces Acting on ship hull under the Lateral Berthing

*Yun-Sok Lee**

**Researcher of Korea Maritime University, Busan, Korea*

Abstract : *In order to keep the safety of maneuverability under the lateral berthing, it is necessary to estimate the magnitudes and properties of the hydrodynamic forces acting on ship hull quantitatively. In this paper, CFD technique is used to calculate the steady lateral force according to the water depth for Wigley model under the unsteady lateral berthing. The numerical results are analysed into the steady lateral force and the transitional lateral force, and some of reviews for the safety of maneuverability relating to the lateral berthing are discussed based on the computed hydrodynamic forces.*

Key words : *Berthing, Steady lateral force, Transitional lateral force, CFD, Safety Maneuverability*

1. Introduction

The berthing problem has been considered as a field of maneuverability, but it is rare on the research of berthing maneuver itself because many recent studies relating to the maneuverability have forced on the coastal and ocean navigation. The berthing maneuver is a specific work that should keep the allowance strength of the mooring facilities as well as the safety of the berthing ship itself. The support of tugboats is compulsory for berthing ship to ensure the safety of mooring facilities. Therefore the motion and the control of berthing ship mainly depend on the tugboats. Also the procedures of berthing seems to be not changed in spited of the quite improvement of maneuverability. Consequently considerable time and effort are still required in a berthing operation. In order to clear these problems in proper, the magnitudes and features of hydrodynamic forces acting on ship hull under the lateral berthing should be evaluated especially in shallow water.

In the work of Sadakane et al.(1996, 1993), the experimental equation is proposed based on the model experiment in deep water. However, the experimental results are restricted to the tanker model and specific water depth. Furthermore the hydrodynamic validity concerning the mechanisms of the hydrodynamic force is required. In the theoretical study, CFDM(Cross Flow Drag Methods, Kijima, 1993) has been used most commonly in the field of maneuverability. However, CFDM assumes that the flow is the two dimensional flow for each cross section. Therefore the magnitude and strength of the separated vortex must be specified at the outer boundary of ship hull, and hydrodynamic forces under the unsteady motion cannot be solved directly with the real time.

Recently computational fluid dynamic(CFD) is become one of the popular tools in analysis and design for application of the ship hydrodynamics and many other branches of fluid mechanics. Chen and Patel(1996, 1998) developed the numerical methods solving the berthing problem. Results presented for several berthing conditions indicated that many important features of the flow were adequately simulated. But the hydrodynamic forces acting on ship hull was not shown. The hydrodynamic forces and transitional lateral force under the lateral berthing have been investigated recently by Toda et al.(2002) in a shallow water using the CFD method for berthing simulation.

In the present study, the previous numerical method(Y. S. Lee, 2003) applied to calculate the steady lateral force according to the water depth. The computed results are analysed into the transitional lateral force and steady lateral force, and the influence of water depths is investigated comparing the both of lateral force. The steady lateral force is an important element to modelize the transitional lateral force and to understand the flow field about the steady conditions. The characteristics of steady lateral coefficient are discussed. Finally, some of reviews for the safety of maneuverability relating to the lateral berthing are mentioned in view of the hydrodynamic characteristics.

2. Numerical methods

The berthing velocity of a large tanker assisted by tugboat in harbor is usually less than 0.15m/s, and the

* Corresponding Author : Yun-Sok Lee, lys@bada.hhu.ac.kr, 051)410-4863

Froude Number Fn determined by taking the ship breadth is very small values. Berthing velocity of deadweight 47,000ton is shown in Fig. 1. Based upon these facts, influence of the free surface was neglected on the computation. The motion mode of berthing simulation is started from the rest to the uniform movement through the constant acceleration.

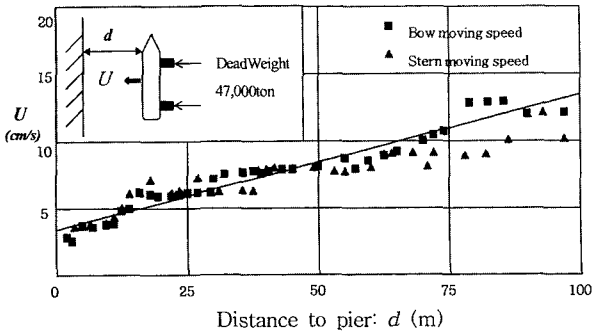

Fig. 1 Example of berthing velocity

2.1 Governing equations and turbulence model

The governing equations are the continuity and 3D Naiver-Stokes equations for viscous incompressible flow written in the physical domain using Cartesian coordinate fixed on the ship hull.

$$\frac{\partial u}{\partial t}+u\frac{\partial u}{\partial x}+v\frac{\partial u}{\partial y}+w\frac{\partial u}{\partial z}=-\frac{\partial P}{\partial x}+\frac{1}{Rn}\left(\frac{\partial^2 u}{\partial x^2}+\frac{\partial^2 u}{\partial y^2}+\frac{\partial^2 u}{\partial z^2}\right)+\frac{dU_0}{dt}$$

$$\frac{\partial v}{\partial t}+u\frac{\partial v}{\partial x}+v\frac{\partial v}{\partial y}+w\frac{\partial v}{\partial z}=-\frac{\partial P}{\partial y}+\frac{1}{Rn}\left(\frac{\partial^2 v}{\partial x^2}+\frac{\partial^2 v}{\partial y^2}+\frac{\partial^2 v}{\partial z^2}\right)$$

$$\frac{\partial w}{\partial t}+u\frac{\partial w}{\partial x}+v\frac{\partial w}{\partial y}+w\frac{\partial w}{\partial z}=-\frac{\partial P}{\partial z}+\frac{1}{Rn}\left(\frac{\partial^2 w}{\partial x^2}+\frac{\partial^2 w}{\partial y^2}+\frac{\partial^2 w}{\partial z^2}\right)$$

$$\frac{\partial u}{\partial x}+\frac{\partial v}{\partial y}+\frac{\partial w}{\partial z}=0 \qquad (1),\ (2),\ (3),\ (4)$$

where Rn is the Reynols numbers, dU_0/dt is the non-dimensional acceleration. All variables are normalized with the breadth B, the reference velocity U_∞ (the uniform velocity), fluid density ρ, and combination of these factors. The SGS (Sub-Grid Scale) turbulence model seems to be suitable for the unsteady and complicated flow field with the shedding vortex and relatively rough computational grid. In the present work, the SGS model adapted taking the eddy viscosity by Smagorinsky and the length scale is determined by Takakura's length scale(Takakura et al., 1989). The non-dimensional equations are transformed into the computational domain in non-orthogonal curvilinear coordinate. A partial transformation is used in which only the independent variables are transformed. Each equation is generally rewritten in the form of the convection/diffusion equation as follows:

$$\frac{1}{J}\sum_{i=1}^{3}\sum_{j=1}^{3}\frac{\partial}{\partial \xi^i}\left(b_i^j U_j\right)=0 \qquad (5)$$

$$\sum_{i=1}^{3}\sum_{j=1}^{3}g^{ij}\frac{\partial^2\phi}{\partial\xi^i\partial\xi^j}-2\sum_{j=1}^{3}a_\phi^j\frac{\partial\phi}{\partial\xi^j}=R_\phi\frac{\partial\phi}{\partial\tau}+S_\phi \qquad (6)$$

The geometric coefficients b, g and J appearing in the above equationa are defined in Patel et al(1990).

The transport equations are discretized using the 12 point FAM(finite analytic method, Patel et al., 1990) as shown in Fig. 2. In the FA scheme, the equation is linearlized in each local numerical elements and solved analytically by the method of separation of variables. Euler implicit method is applied to the time derivatives. Pressure-velocity coupling is accomplished using the PISO(Pressure Implicit Split Operator) algorithm(Chen, 1993). Therefore hundred times of repetition are required for every trial of the calculation of one-time step, the coefficient of the FA method was renewed every time repetition.

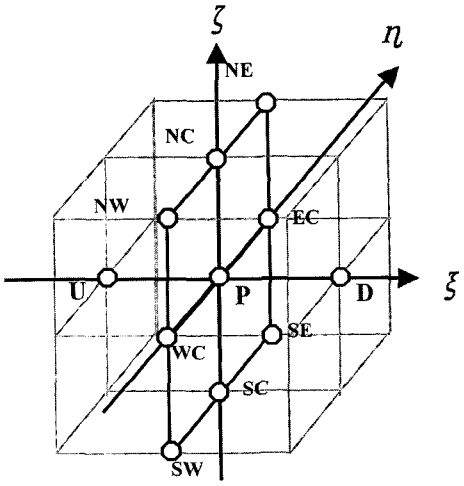

Fig. 2 Grid arrangement using 12-points FA methods

2.2 Computational grid and boundary conditions

Table 1 shows the principal particulars of Wigley model. Length and draft are normalized by ship's breadth. The present computational grid is H-type with constant Y planes, which is generated by solving the Possion equation. Coordinate system and computational grid of Wigley hull is shown in Fig. 3. The origin is at the water surface and midship section. X is the opposite direction for the movement, Y is the ship length direction and Z is directed vertically upward.

Table 1 Particulars of the Wigley model

Type	Wigley model
Length (L)	10.0
Breadth (B)	1.0
Draft (d)	0.625
Block Coefficient C_b	0.444

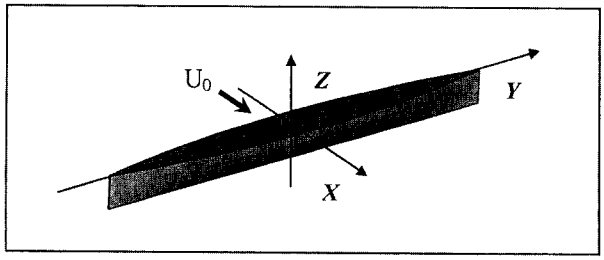

Fig. 3 The coordinate system and body shape

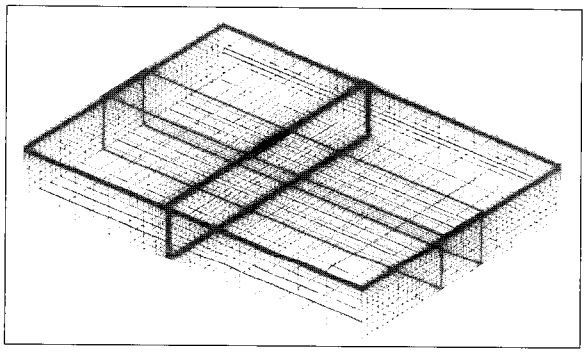

Fig. 4 Global view of computational grid

The computational gird number is 81×95×35 in directions of X, Y, and Z in case of the deep water region. When H/d is 2.0 and 1.5, computation grid was conducted by reducing exclusively the Z axis to 19 and 21, respectively. Fig.4 shows global view of computational grid. The boundary condition is given in the shallow water region as follows: the inlet boundary condition (x = -30); $u = U_0$, $v = w = p = 0$, the outlet boundary condition (x = 30, 0 extrapolation); $\partial u/\partial x = \partial v/\partial x = \partial w/\partial x = \partial p/\partial x = 0$, the side(right and left) boundary condition (y = 25); $u = U_0$, v = w = p = 0. Furthermore the boundary condition on the hull surface was approximated with $u = v = w = 0$, $\partial p/\partial x = dU_0/dt$. Body hull is located $-5 \leqq y \leqq 5$, $-0.5 \leqq x \leqq 0.5$. Non-dimensional acceleration for computation is 1 ($dU_0/dt = 1$). The Reynolds number was designated as 10^5 considering the Reynolds number of the experiment, and the non-dimensional time interval of 1 step is Δt = 0.005 (200 steps are equivalent to the non-dimensional time T=1.0)

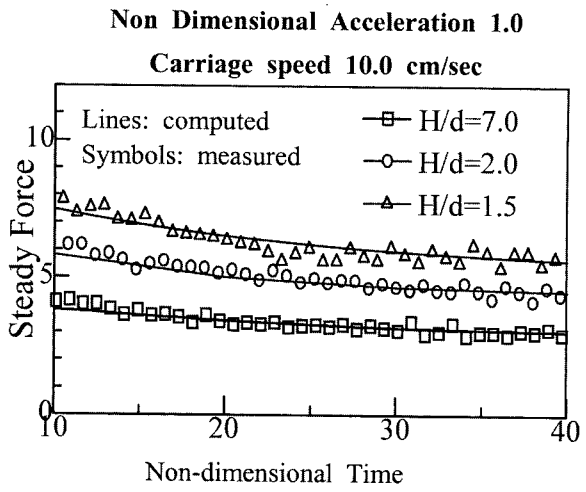

Fig. 5 Comparison of the computed and measured lateral force according to the water-draft ratio

3. Results and discussion

3.1 Steady lateral force according to the water depth

The comparison of lateral force between computations and experiments according to the water depth, such as H/d=2.0, 1.5 and H/d=7.0 is shown in Fig. 5. The force F and the moving velocity U_0 are the normalized values, and the non-dimensional acceleration is 1.0. The solid line gives the computation result, whereas the dotted line gives the experimental result obtained by using a lateral force measurement device. In order to compare both of the hydrodynamic forces directly, inertia force corresponding to the model mass used in the experiment was added to the CFD result. The experimental result is obtained by using the equipment of lateral force measurement with a servo motor control, as shown in Fig. 6. The equipment can be set the carriage speed and acceleration freely on the personal computer. The CFD result coincides with the experimental result. T=10.0~T=40.0 is the uniform movement of ship hull. One of the hydrodynamic features caused by the difference of the water depth is that the steady lateral force at T=30.0 shows largely as the force comes to shallower water. The steady force of H/d=1.5 is 2.4 times larger than that of H/d=7.0 at T=20.0. Also, there are big differences between the transitional lateral force after T=10.0 and the steady lateral force around the T=30.0. It is interesting note that the time of steady condition is considerably different on the water depths. In case of H/d=7.0, the time of steady condition seems to be around T=22.0, but it takes more time when H/d is 1.5.

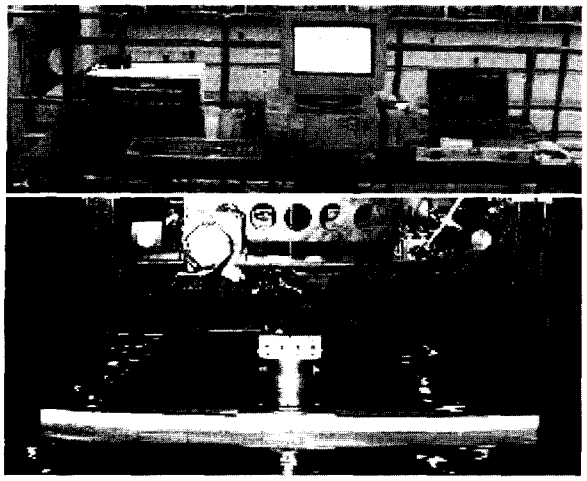

Fig. 6 Experimental set-up and PC control servo-motor

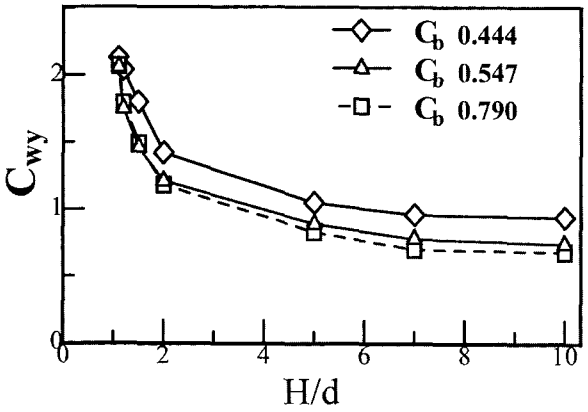

Fig. 7 Comparison of steady lateral force coefficients

In order to analyze a more detailed characteristics of the steady lateral force, the computed results are transformed into the steady lateral coefficients($C_{wy}=F/0.5L\,d\,U_0^2$) as shown in Fig.7. Fig.7 presents the influence of water depths on the steady lateral coefficients. The several experimental data of other ship forms are included in the figures. The symbols(◇, △, □) of several experimental data show the Wigley ship(C_b =0.444), Tanker ship(C_b =0.79) and PCC ship(C_b =0.547), respectively. It is commonly seen that the steady lateral coefficients sharply increase under the range of H/d=3.0 and there is no change over the range of H/d=7.0. It is further noted that the coefficients of Wigley ship is larger than that of tanker ship forms in deep water, but the trends is reversed in shallow water region. The coefficients ratio(shallow water lateral coefficients/deep water lateral coefficients) of Wigley ship shows 2.01 when H/d is1.1. On the other hand, the coefficients ratio of tanker ship is 2.83. From these results, the ship with large block coefficients are influenced more than small ones in the shallow water, but this needs further investigation.

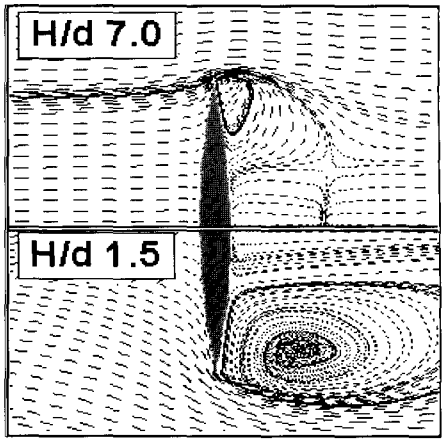

Fig. 8 Comparison of surface streamlines

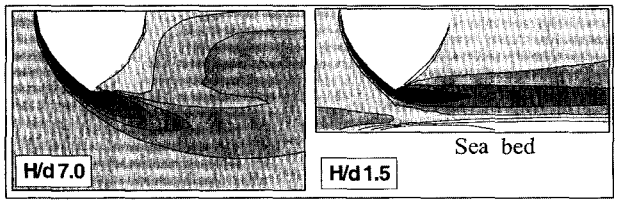

Fig. 9 Comparison of vortex distribution

3.2 Visualization of steady conditions

Fig. 8 shows the streamlines of water surface plane in case of H/d=7.0 and 1.5 at T=30.0. It is found that the flow patterns in deep water are considerably different from those observed in shallow water especially at the wake region. In case of shallow water, since the flow comes to be hard to go through the ship bottom, a flow recirculating around the bow and stern appears remarkably. Also strong vortical flows adjacent to the ship hull are observed in shallow water. Therefore great pressure is worked on the hull especially in a shallow region. Fig. 9 shows the vorticity distribution(ω = rot u) of steady conditions at midsection. It is clear that the shape of vortex region behind the hull body in deep water is different from those observed in shallow water. In case of deep water, the shedding vorticies are moved to the downstream freely, and make the wake region. However, the shedding vorticies from keel are restricted by the presence of sea floor in shallow water, also are moved to the horizontally and make the narrow band wake region. Furthermore, the strength of the shedding vortex in shallow water is also considerably larger than that obtained in deep water. It is interesting to note that the lateral motion of ship induced opposite vertex to the wake region on the sea floor.

From the visualized information(Fig. 8), (Fig. 9), the influence on the flow field around the ship hull can be

easily explained. Thus it can be ensured that the water depth is an important element to affect in fluence on the hydrodynamic force, and it has become possible to compare and examine the hydrodynamic force in detail by means of CFD method.

4. The safety of berthing maneuver

The purpose of the previous(Lee, 2003) and this study is to understand the hydrodynamic characteristics and physical phenomena, and to enhance the safety of berthing maneuver. There are many environmental elements, which should be considered the berthing problems, such as the topology of harbor, water depth, wind and current. Also, it is impossible to standardize the berthing maneuver due to the various of ship types and environmental elements. However the components of hydrodynamic force acting on ship hull under the lateral berthing are same as like the inertia force and lateral force. It is worthwhile that some of reviews for the safety of berthing maneuver are discussed from the aspects of the obtained hydrodynamic forces.

From the hydrodynamic aspects, the safety of berthing maneuver can be described as follows:

1) It is desirable that the inertia force induced by the accelerations motion should be minimized by refraining the use of tugboat. Furthermore, the sudden use of tugboat must be avoided especially in front of mooring facilities and pier as possible.
2) The departing ship could be slowly pulled by the tugboat, which can reduce the inertial force and prevent the breakdown of mooring rope as well.
3) The ship moving within the short time must be avoided because the transitional lateral force works large.
4) There are many cases that the berthing ship is usually stopped and pushed by the tugboat ensuring the safety of the mooring facilities. However, if there are no obstacles around the berthing area and the strength of mooring facilities is allowed. It is more effective to keep the small constant berthing speed for reduction of the berthing energy without the temporary stop.
5) The one of ways for minimizing the berthing energy and the maximizing the berthing operation is that the berthing speed keeps constant considering the berth allowance of structure strengthening.
6) Water depth is an important factor to influence on the hydrodynamic forces, so berthing operation should be executed making sure of enough under keel clearance.

5. Conclusion

The numerical computation using CFD was performed for Wigley model undergoing the lateral berthing in open seas. The results of this paper can be summarized as the following:

1) The availability and validity of CFD technique for the berthing simulations is verified.
2) The numerical solutions successfully captured not only the characteristics of the steady lateral force but also some interesting features of the flow field.
3) The steady lateral forces were worked on 2.04 times H/d=1.5 in shallow water more then H/d=7.0 in deep water.
4) Some of reviews for the safety of berthing maneuver are described based on the aspects of the obtained hydrodynamic forces.

The result of this research is expected to play a role in providing the hydrodynamic understanding for ship operator, designing the of fenders and determining the strength of mooring facilities.

References

[1] Chen, H. C. and Korpus, R.(1993) "A Multi-block Finite-Analytic Reynolds-Averaged Navier-Stokes Method for 3D Incompressible Flows", Individual Papers in Fluid Engineering, edited b F. M. White, ASME FED-Vol. 150, ASME Fluids Engineering Conference, pp. 113-121.

[2] Chen, M. and Chen, H. C.(1996) "Numerical Simulation of Transient Flows Induced by a Berthing Ship", International Journal of Offshore and Polar Engineering, ISOPE, Vol. 7, No.4, pp. 277-284.

[3] Chen, M. and Chen, H. C.(1998) "Chimera RANS Simulation of a Berthing DDG-51 Ship in Translational and Rotational Motions", International Journal of Offshore and Polar Engineering, Vol. 8, No.3, pp. 182-191.

[4] LEE, Y. S.(2003) "The Prediction of Hydrodynamic Forces Acting on Ship Hull in Laterally Berthing Maneuver Using CFD", International Journal of Navigation and Port Research, Vol. 27, No34, pp. 253-258.

[5] Patel, V. C, Chen, H. C. and Ju, S.(1990) "Ship Stern and Wake Flows: Solutions of the Fully-Elliptic Reynolds-Averaged Navier-Stokes Equations and Comparisons with Experiments", Journal of Computational Physics, Vol. 88, No.2, pp. 305-336.

[6] Sadakane, H.(1996) "A Study on Lateral Drag Coefficient for Ship Moving Laterally from Rest", Journal of the Japan Institute of Navigation, No. 95, pp. 193-200.

[7] Sadakane, H. and Tsuruta, H.(1993) "Transitional Lateral Drag Acting on Ship Moving from the Rest -An Experimental Study by Using a Ship"s Model-", Journal of the Japan Institute of Navigation, No. 90, pp. 273-279.

[8] Tanaka, H. and Kijima, K.(1993) "On the Distribution of Cross Flow Drag over the Length of a Ship Moving Transversely", The Society of Naval Architects of Japan, No. 174, pp. 1-8.

[9] Toda, Y., Lee, Y. S. and Sadakane, H.(2002) "Hydrodynamic Forces acting on ship hull Under Lateral Low Speed MotionⅢ: Basic Consideration Using 3-D CFD Technique", Journal of the Japan Institute of Navigation, No. 106, pp. 87-95.

[10] Takakura, Y., Ogiwara, S. and Isiguro, T. (1989) "Turbulence Models for Transonic Viscos Flow", AIAA paper, 89-1952 CP.

Received 10 November 2003
Accepted 8 December 2003